Article

Cell Reports

Bimodal CD40/Fas-Dependent Crosstalk between iNKT Cells and Tumor-Associated Macrophages Impairs Prostate Cancer Progression

Graphical Abstract

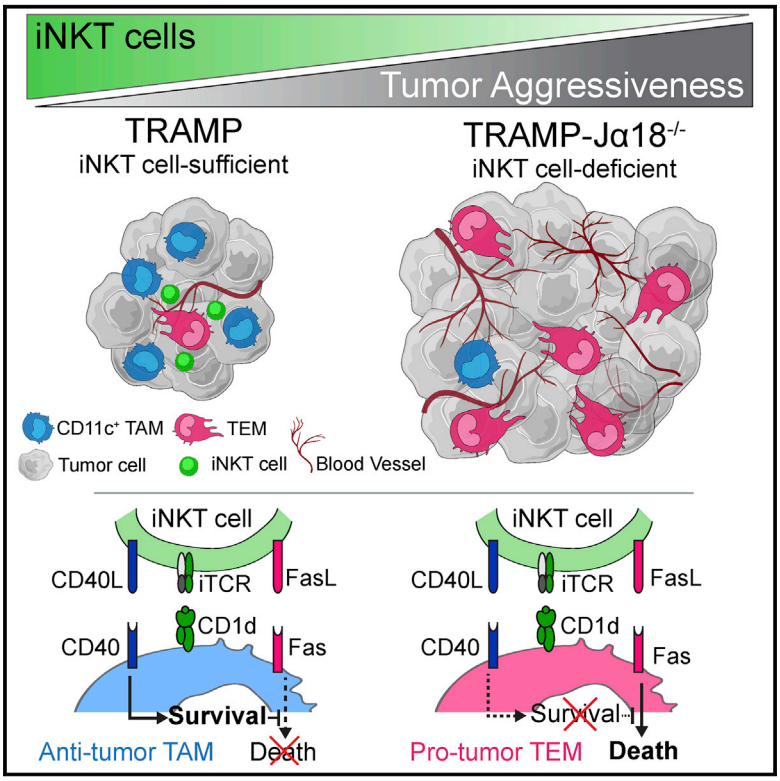

Authors

Filippo Cortesi, Gloria Delfanti, Andrea Grilli, ..., Matteo Bellone, Giulia Casorati, Paolo Dellabona

Correspondence

bellone.matteo@hsr.it (M.B.), casorati.giulia@hsr.it (G.C.), dellabona.paolo@hsr.it (P.D.)

In Brief

Cortesi et al. provide evidence that iNKT cells contribute to cancer immune surveillance. Due to differential tuning of tumor-associated macrophage populations, iNKT cells remodel the microenvironment of prostate cancer, enforcing a tumor-opposing state that controls tumor progression.

Highlights

- iNKT cells remodel the tumor microenvironment of mouse prostate cancer
- iNKT cells restrict pro-angiogenic TEMs and sustain pro-inflammatory TAMs
- iNKT cells differentially modulate TAMs by cooperative CD1d, CD40, and Fas engagement
- Aggressive human prostate cancers contain high TEMs and low iNKT cells

Data and Software Availability

GSE94359

Cortesi et al., 2018, Cell Reports 22, 3006–3020
March 13, 2018
https://doi.org/10.1016/j.celrep.2018.02.058

CellPress

OPEN ACCESS
CellPress

Cell Reports
Article

Bimodal CD40/Fas-Dependent Crosstalk between iNKT Cells and Tumor-Associated Macrophages Impairs Prostate Cancer Progression

Filippo Cortesi,[1] Gloria Delfanti,[1] Andrea Grilli,[2,3] Arianna Calcinotto,[4] Francesca Gorini,[1] Ferdinando Pucci,[5] Roberta Lucianò,[6] Matteo Grioni,[4] Alessandra Recchia,[7] Fabio Benigni,[8] Alberto Briganti,[8] Andrea Salonia,[8,9] Michele De Palma,[10] Silvio Bicciato,[2] Claudio Doglioni,[6,9] Matteo Bellone,[4,*] Giulia Casorati,[1,*] and Paolo Dellabona[1,11,*]

[1]Experimental Immunology Unit, Division of Immunology, Transplantation and Infectious Diseases, San Raffaele Scientific Institute, Milan 20123, Italy

[2]Center for Genome Research Department of Life Sciences, University of Modena and Reggio Emilia, Modena, Italy

[3]PhD Program of Molecular and Translational Medicine, Department of Medical Biotechnology and Translational Medicine, University of Milan, 20090 Segrate, Italy

[4]Cellular Immunology Unit, Division of Immunology, Transplantation and Infectious Diseases, San Raffaele Scientific Institute, Milan 20123, Italy

[5]Torque Therapeutics Inc., Cambridge, MA 02142, USA

[6]Division of Pathology, San Raffaele Scientific Institute, Milan 20123, Italy

[7]Centre for Regenerative Medicine, Department of Life Sciences, University of Modena and Reggio Emilia, Modena, Italy

[8]Division of Experimental Oncology/Unit of Urology, URI, IRCCS Ospedale San Raffaele, Milan 20123, Italy

[9]San Raffaele Vita-Salute University, Milan 20123, Italy

[10]Swiss Institute for Experimental Cancer Research (ISREC), School of Life Sciences, Ecole Polytechnique Fédérale de Lausanne (EPFL), 1015 Lausanne, Switzerland

[11]Lead Contact

*Correspondence: bellone.matteo@hsr.it (M.B.), casorati.giulia@hsr.it (G.C.), dellabona.paolo@hsr.it (P.D.)

https://doi.org/10.1016/j.celrep.2018.02.058

SUMMARY

Heterotypic cellular and molecular interactions in the tumor microenvironment (TME) control cancer progression. Here, we show that CD1d-restricted invariant natural killer (iNKT) cells control prostate cancer (PCa) progression by sculpting the TME. In a mouse PCa model, iNKT cells restrained the pro-angiogenic and immunosuppressive capabilities of tumor-infiltrating immune cells by reducing pro-angiogenic TIE2$^+$, M2-like macrophages (TEMs), and sustaining pro-inflammatory M1-like macrophages. iNKT cells directly contacted macrophages in the PCa stroma, and iNKT cell transfer into tumor-bearing mice abated TEMs, delaying tumor progression. iNKT cells modulated macrophages through the cooperative engagement of CD1d, Fas, and CD40, which promoted selective killing of M2-like and survival of M1-like macrophages. Human PCa aggressiveness associate with reduced intra-tumoral iNKT cells, increased TEMs, and expression of pro-angiogenic genes, underscoring the clinical significance of this crosstalk. Therefore, iNKT cells may control PCa through mechanisms involving differential macrophage modulation, which may be harnessed for therapeutically reprogramming the TME.

INTRODUCTION

Tumors contain malignant cells embedded in a complex microenvironment comprising non-transformed stromal cells, neovasculature, and immune cells, whose crosstalk controls tumor progression (Hanahan and Coussens, 2012). Deciphering the cellular and molecular interactions in the tumor microenvironment (TME) may provide new targets for improving anticancer therapies (Hanahan and Weinberg, 2011). Macrophages frequently make up a sizable proportion of the immune cell compartment of tumors (Mantovani et al., 2002). Tumor-associated macrophages (TAMs) largely derive from circulating monocytes (Franklin et al., 2014), which acquire in the TME both tumor-promoting and antagonizing functions encompassing immune suppression and surveillance, the regulation of angiogenesis, and the facilitation of cancer cell invasion and metastasis (Noy and Pollard, 2014). Although the dichotomous distinction between M1 (pro-inflammatory and immunostimulatory) and M2 (pro-angiogenic and pro-tumoral) TAMs may oversimplify macrophage complexity (Mantovani et al., 2002; Murray et al., 2014), it can fairly identify phenotypically and functionally discrete TAM subsets that populate distinct TMEs (Noy and Pollard, 2014; Squadrito et al., 2012). For example, Tie2-expressing macrophages (TEMs) express a marked M2-like molecular signature (Pucci et al., 2009) and have pro-angiogenic, immunosuppressive, and pro-metastatic functions (Lewis et al., 2016). Conversely, CD11c$^+$/Tie2-negative TAMs express a M1-skewed gene signature and exhibit angiostatic and immunostimulatory functions (Baer et al., 2016; Pucci et al., 2009).

Invariant natural killer T (iNKT) cells are a T lymphocyte subset with innate effector functions and a conserved semi-invariant T cell receptor (TCR) restricted to the major histocompatibility complex (MHC) class I-related CD1d molecule (Brennan et al., 2013). iNKT cells recognize a range of microbial lipids but are also self-reactive against endogenous lipids that are upregulated under stress conditions (Brennan et al., 2013). Upon activation, iNKT cells modulate the functions of other innate and adaptive immune effector cells via direct contact and cytokine production (Brennan et al., 2013).

iNKT cells have been implicated in the control of infectious pathogens, autoimmunity, and cancer progression (Brennan et al., 2013). In animal models, activation of iNKT cells by the administration of CD1d-restricted antigens, such as the synthetic glycosphingolipid α-galactosyl-ceramide (αGalCer), promotes potent antitumoral immune responses via dendritic cell (DC) licensing, production of immunostimulatory interferon-γ (IFNγ) and interleukin-12 (IL-12), and recruitment of cytotoxic $CD8^+$ T and NK cells (Hayakawa et al., 2001; Hermans et al., 2003; Nakagawa et al., 2001). Moreover, αGalCer-mediated IFNγ secretion by iNKT cells impairs tumor angiogenesis (Hayakawa et al., 2002). iNKT infiltration is a positive prognostic factor in neuroblastoma and colorectal cancer (Metelitsa et al., 2004; Tachibana et al., 2005), whereas low iNKT numbers or unresponsiveness are reported in patients with different types of advanced malignancy (Dhodapkar et al., 2003; Tahir et al., 2001). Low circulating iNKT numbers predict poor outcome in patients with head-and-neck squamous carcinoma (Schneiders et al., 2012) and progression of chronic lymphocytic leukemia (Gorini et al., 2017) and also correlate with leukemia relapse in patients following stem cell transplantation (de Lalla et al., 2011). In mouse cancer models, iNKT cells play an important role in immune surveillance against different tumor types (Bassiri et al., 2014; Bellone et al., 2010; Crowe et al., 2002; Renukaradhya et al., 2008; Swann et al., 2009), which depends on the direct recognition of CD1d-expressing malignant cells (Bassiri et al., 2014; Renukaradhya et al., 2008) or indirect mechanisms, such as IFNγ-dependent enhancement of cytotoxic $CD8^+$ T and NK cell responses (Crowe et al., 2002), modulation of immunosuppressive myeloid cells (De Santo et al., 2010), or killing of TAMs (Song et al., 2009).

We have previously shown that genetic impairment of iNKT cells in the oncogene-driven TRAMP prostate cancer (PCa) model (Greenberg et al., 1995) accelerated and aggravated tumorigenesis without affecting tumor-specific $CD8^+$ T cells (Bellone et al., 2010). In this study, we document that iNKT cells control PCa progression by restricting protumoral TEMs and supporting antitumoral $CD11c^+$ TAMs via non-redundant mechanisms entailing the cooperative engagement of CD1d, Fas, and CD40.

RESULTS

Absence of iNKT Cells Subverts the TRAMP PCa Microenvironment

Our previous data implicated iNKT cells in the control of PCa progression in iNKT-deficient TRAMP-Jα18$^{-/-}$ mice (Bellone et al., 2010). To rule out immunosuppressive or tumor-promoting functions of CD1d-restricted type-II NKT cells (Godfrey et al., 2010), which are present in TRAMP-Jα18$^{-/-}$ mice, we here generated TRAMP-CD1d$^{-/-}$ mice lacking all CD1d-restricted NKT cells. As shown in Figure 1A, both TRAMP-Jα18$^{-/-}$ and TRAMP-CD1d$^{-/-}$ mice had similarly shortened survival compared with TRAMP mice, suggesting that iNKT cells are the only CD1d-dependent cells involved in the control of TRAMP-PCa progression.

Earlier work failed to identify differences in cytotoxic T lymphocyte (CTL) responses against the PCa-associated antigens TagIV, PSCA, and STEAP between iNKT-proficient and deficient TRAMP mice (Bellone et al., 2010). We therefore hypothesized that iNKT cells could control PCa progression through effects on the TME. We characterized the impact of iNKT cells on the molecular pathways expressed by TRAMP PCa-infiltrating immune cells at different stages of progression. We sorted $CD45^+$ hematopoietic cells from the prostate of TRAMP and TRAMP-Jα18$^{-/-}$ mice at 8, 12, and 16 weeks of age and compared their gene expression profiles. Gene set enrichment analysis (GSEA) identified multiple pathways that were differentially modulated in at least one time point, with 12 significantly modulated at all analyzed time points (Figure S1). Notably, in the absence of iNKT cells, the *interferon alpha response* and *interferon gamma response* gene sets were significantly downregulated, whereas the *hallmarks angiogenesis* gene set was significantly enriched (Figure 1B). Accordingly, we observed increased $CD31^+$ vascular areas in the prostate of TRAMP-Jα18$^{-/-}$ mice compared to age-matched TRAMP mice (Figures 1C and 1D). Consistent with previous data (Bellone et al., 2010), the prostates of TRAMP-Jα18$^{-/-}$ mice contained larger $SV40^+$ malignant epithelial cell areas than those of TRAMP mice (Figures 1C and 1E).

The above results prompted us to examine myelo-monocytic cells in TRAMP and TRAMP-Jα18$^{-/-}$ PCa, including myeloid-derived suppressor cells (MDSCs), TAMs, and DCs (Gabrilovich et al., 2012), all of which are known to regulate angiogenesis (De Palma et al., 2017). As shown in Figures 2A–2C, unsupervised high-dimensional flow cytometry analyses identified differences in the TAMs ($CD45^+F4/80^{high}CD11b^+Gr\text{-}1^-$) of TRAMP and TRAMP-Jα18$^{-/-}$ mice. In the absence of iNKT cells, macrophages with a TEM phenotype ($MRC1^+CD11c^-$) were increased, whereas macrophages with an M1-like, pro-inflammatory phenotype ($CD11c^+MRC1^-$) were decreased (Figures 2A–2C). The other examined immune cell subsets were found at similar frequencies in the two genotypes. TEMs were the only cell population expressing high levels of MRC1, whereas pro-inflammatory TAMs expressed CD11c in combination with high-level F4/80 and CD11b and variable levels of MHCII (Figure 2C). Analytical flow cytometry analyses confirmed that TEMs were significantly increased, whereas $CD11c^+$ TAMs were reduced in the prostates of 10-week-old TRAMP-Jα18$^{-/-}$ mice (Figure 2D). Thus, absence of iNKT cells increased the TEM/$CD11c^+$ TAM ratio in PCa (Figure 2E). Histological analysis revealed increased accumulation of $F4/80^+$, MRC1-expressing TEMs in the stroma of the prostatic lobes of TRAMP-Jα18$^{-/-}$ mice between 10 and 25 weeks of age (Figures 2F and 2G). Interestingly, this trend was not observed in iNKT-proficient TRAMP prostates (Figure 2H). Collectively, these results suggested a

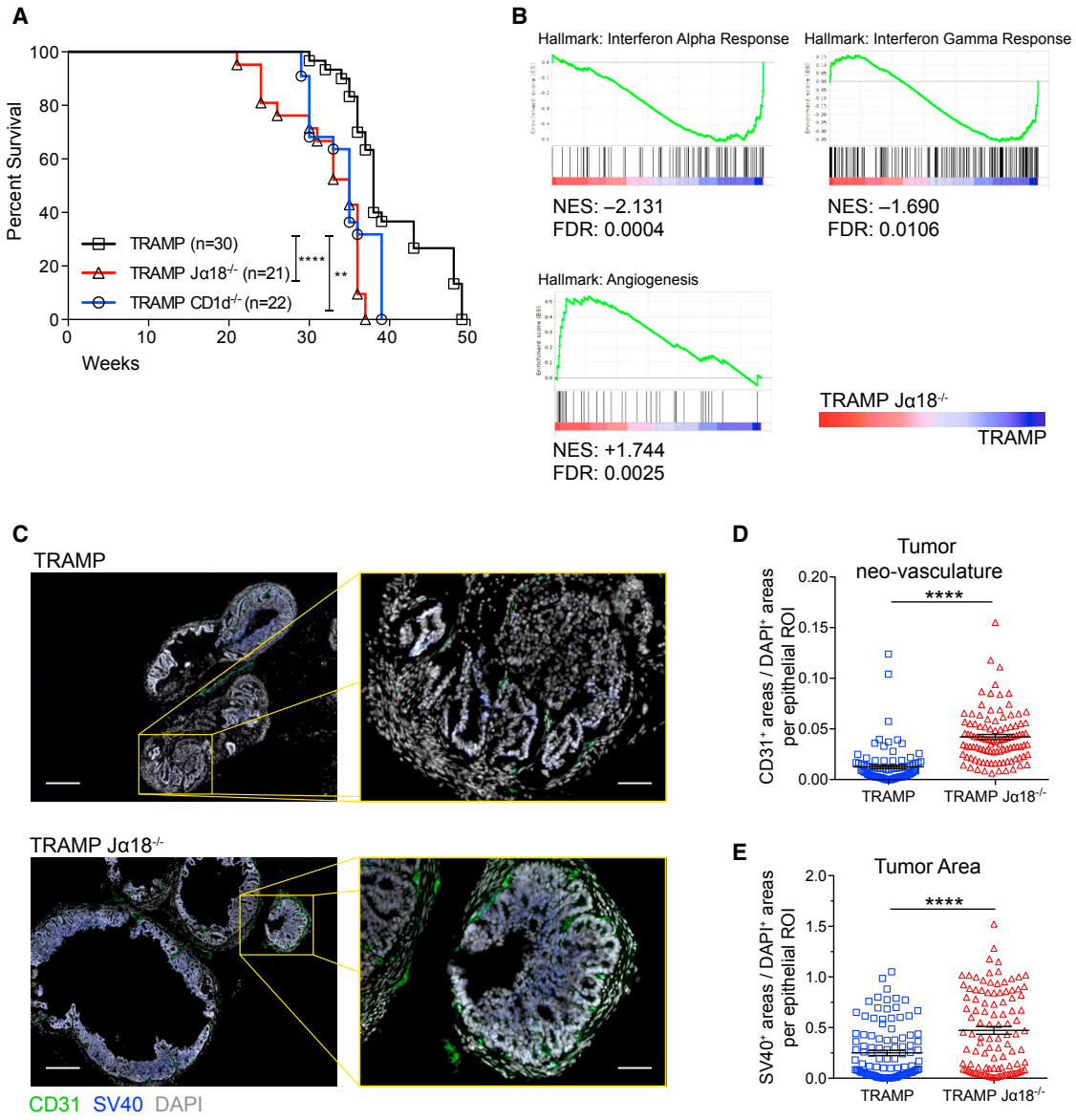

Figure 1. Absence of iNKT Cells Reduces TRAMP Mice Survival and Alters Prostate Cancer Microenvironment

(A) Kaplan-Mayer survival analysis of male TRAMP (n = 30), TRAMP Jα18$^{-/-}$ (n = 21), and TRAMP-CD1d$^{-/-}$ (n = 22) mice.

(B) Differential GSEA enrichment plots of the indicated gene sets in TRAMP-Jα18$^{-/-}$ versus TRAMP tumors at 12 weeks.

(C) Representative immunofluorescence staining for vascular endothelial cells (CD31, green), tumor cells (SV40, blue), and nuclei (DAPI, gray) in 25-week-old TRAMP and TRAMP-Jα18$^{-/-}$ prostates. Bars represent 200 μm (left panels) and 50 μm (right panels). Tissues were from >3 independent mice per strain.

(D and E) Quantification of (D) CD31^{+} tumor vascular and (E) SV40^{+} tumor areas in prostates of indicated mice. Dots represent CD31^{+} or SV40^{+} cell areas normalized on DAPI signal in a single tumor area. 15 random non-overlapping fields per slide were analyzed.

Statistical analysis by log rank test corrected for multiple comparisons (A) and Student's two-tailed t test (D and E). Bars in (D) and (E) indicate mean ± SEM. See also Figure S1.

critical role for iNKT cells in modulating TAM subpopulations in the PCa microenvironment of TRAMP mice.

iNKT Cell Transfer Decreases TEMs and Delays PCa Progression

To study iNKT function, we adoptively transferred iNKT cells from healthy C57BL/6 animals into TRAMP-Jα18$^{-/-}$ male mice at about 7 weeks of age and examined TEMs and CD11c^{+} TAMs in their prostates 3 weeks later. iNKT cell transfer into TRAMP-Jα18$^{-/-}$ mice significantly abated TEM frequency (Figure 3A) and absolute numbers (Figure S2A) to levels observed in age-matched TRAMP mice. At variance, CD11c^{+} TAMs remained unaffected (Figure S2B).

To investigate the functional involvement of iNKT cells in TAM programming and PCa progression, we used a transplant model. We inoculated TRAMP-C1 PCa cells subcutaneously into

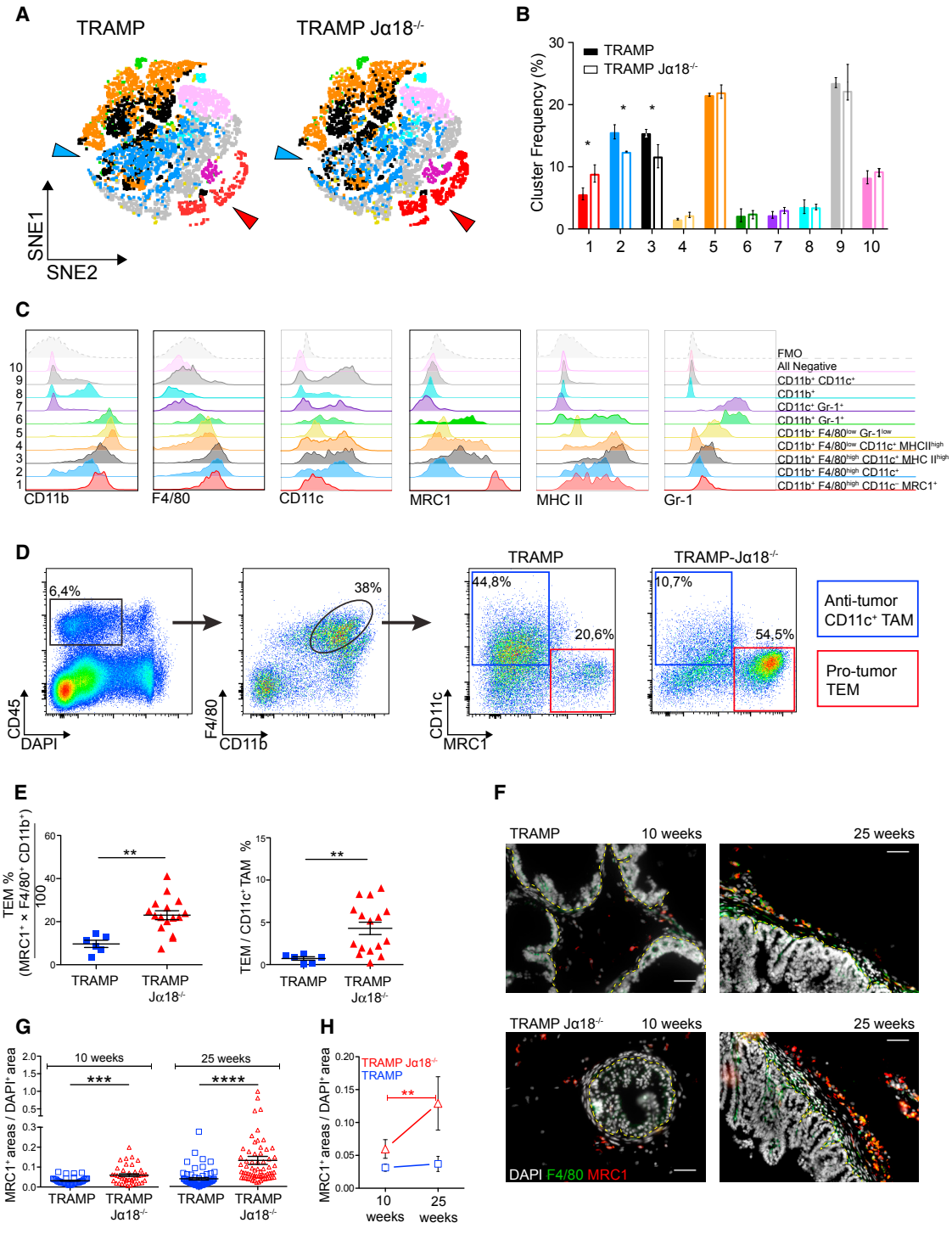

Figure 2. Absence of iNKT Cells in TRAMP Mice Subverts TAM Populations

(A) High-dimensional tSNE maps of prostate-infiltrating myelo-monocytic cells of indicated mice. Representative maps from one mouse/strain are shown, each clustered in 10 populations. Arrowheads indicate major differences in blue and red populations between the two strains.

(B) Comparative frequency of each cluster between TRAMP and TRAMP-Jα18$^{-/-}$ PCs.

(C) Expression of every marker in each cluster to define their specific phenotype (indicated on the right column). Dashed histograms show fluorescence minus one controls.

(D) Representative flow cytometry identification of MRC1^{+}TEMs and CD11c^{+}TAMs in the prostate-indicated mice.

(legend continued on next page)

C57BL/6 or Jα18$^{-/-}$ mice, followed by adoptive iNKT cell transfer either 24 hr or 20 days later. Consistent with data obtained in the autochthonous TRAMP PCa model, the progression of TRAMP-C1 tumors was accelerated in Jα18$^{-/-}$ mice (Figure 3B). Also, both TEM frequency and TEM/CD11c^{+} TAM ratio were significantly increased in TRAMP-C1 tumors growing in the iNKT-deficient hosts (Figures 3C and 3D). Remarkably, iNKT cell transfer significantly delayed tumor progression (Figure 3B) and restored unaltered TEM frequency and TEM/CD11c^{+} TAM ratio (Figures 3C and 3D) in iNKT-deficient mice.

To further study the links between iNKT cells and TAMs in the control of PCa progression, we used an anti-CSF1 receptor (CSF1R) monoclonal antibody (mAb) to eliminate TAMs. CSF1R blockade efficiently eliminated most of the TAMs (Figures S2C–S2F), with the residual cells displaying a CD11c^{+}MRC1^{-} pro-inflammatory phenotype (Figure S2D). TAM elimination significantly decreased intraepithelial neovascularization (Figures 3E and 3F) and the extension of SV40^{+} tumor areas (Figure 3G) in TRAMP-Jα18$^{-/-}$ prostates. It also effectively eliminated TAMs in transplanted TRAMP-C1 tumors of wild-type (WT) mice (Figure S2G) and significantly delayed tumor progression in iNKT-proficient mice (Figure 3H). These results suggest a functional link between the presence of iNKT cells, the modulation of pro-angiogenic TEMs, and the control of PCa progression in TRAMP mice.

iNKT Cells Localize and Operate in the TME

We next asked whether iNKT cells control PCa progression directly in the TME. We first assessed the presence of iNKT cells in the prostates of TRAMP mice by flow cytometry. As shown in Figure 4A, sizeable quantities of iNKT cells were detected in the TRAMP prostates at different disease stages, consistent with previous studies (Nowak et al., 2010). The relative abundance of prostate-infiltrating iNKT cells remained unchanged in aging WT mice but increased in TRAMP mice (Figures S3A and S3B) along with tumor-infiltrating CD45^{+} cells (Figure S3C) and tumor volume (Figure S3D). Notably, most iNKT cells had a iNKT1 effector phenotype, whereas only a minority had a iNKT17 phenotype. The relative frequency of the two subsets varied with time in TRAMP, but not in healthy prostates, suggesting a dynamic turnover of effector iNKT cell subsets associated with tumor progression (Figure 4B). Similar changes in the iNKT1/iNKT17 subset ratio were also detected in inguinal lymph nodes, but not in liver and spleen, of TRAMP mice (Figure S3E). Upon *ex vivo* analysis, iNKT cells of TRAMP prostates (8 weeks of age) displayed effector cytokine profiles similar to iNKT cells of normal prostates. In all samples, iNKT17 only produced IL-17, whereas iNKT1 cells mainly produced IFNγ (Figure 4C).

Next, we determined iNKT cell localization in the tumor tissue by staining TRAMP PCa sections with CD1d tetramers. iNKT cells co-localized with TEMs in the stroma surrounding cancer-containing prostate acini but were not observed in epithelial areas of TRAMP prostates; as expected, iNKT cells were absent in TRAMP-CD1d$^{-/-}$ mice (Figures 4D and S4A). The overall abundance of iNKT cells in the prostate, determined by histo-cytometry analysis on tissue sections, was consistent with that determined by flow cytometry of single-cell suspensions (Figures 4E and S4B). Of all iNKT cells examined by microscopy in TRAMP prostates, >80% were in close proximity to MRC1^{+} TEMs (Figure 4F). Confocal analysis further revealed close association between iNKT cells and TEMs in the PCa stroma (Figures 4G and 4H). To corroborate these findings, we examined whether adoptively transferred iNKT cells could infiltrate the prostate of TRAMP-Jα18$^{-/-}$ mice to contact TEMs. Confocal imaging showed CD1d-tetramer^{+} cells in the prostate of TRAMP-Jα18$^{-/-}$ mice as early as 3 days after adoptive iNKT cell transfer (Figure 4I). As the endogenous iNKT cells, the transferred cells also home to and interact with TEMs. The ability of adoptively transferred iNKT cells to home to the prostate of TRAMP-Jα18$^{-/-}$ mice was confirmed by retrieving fluorescently labeled cells from prostate tissue (Figure S5A). To explore whether functional iNKT/macrophage interactions also occur in the spleen of tumor-bearing mice (Cortez-Retamozo et al., 2012), we splenectomized TRAMP-Jα18$^{-/-}$ mice at 4 weeks of age and, 3 weeks later, transferred iNKT cells to half of them. Splenectomy did not perturb the PCa microenvironment, as both sham-operated and splenectomized TRAMP-Jα18$^{-/-}$ mice had comparable TEMs/CD11c^{+} TAMs proportions, which were decreased by iNKT cell transfer (Figure S5B). Collectively, these results lend strong support to a direct iNKT cell action on TAMs at the tumor site.

iNKT Cells Differentially Modulate TAM Subpopulations through Non-redundant Mechanisms

To unravel the mechanisms by which iNKT cells modulate TAMs in the TRAMP PCa model, we examined putative modes of iNKT/TAM interaction. We hypothesized three different, not mutually exclusive mechanisms: (1) CD1d-dependent interaction between the two cell types; (2) TAM modulation/differentiation via CD40L-CD40 engagement or IFNγ production by iNKT cells; and (3) TAM killing by FasL-Fas engagement. Of note, CD40 engagement by iNKT cells enhances antitumor and antiviral immunity by promoting DC maturation and IL-12 production (De Santo et al., 2008; Kitamura et al., 1999). IFNγ is a major inducer of antitumor M1-like cells, and its baseline or αGalCer-induced production by iNKT cells inhibits sarcoma growth and

(E) Differential TEM frequency (left panel) and TEM/ CD11c^{+}TAM ratio (right panel), calculated by normalizing the percentage of MRC1^{+} or CD11c^{+} cells on the frequency of F4/80^{high}CD11b^{+} cells. Dots represent single mice.

(F) Immunofluorescence staining for TEMs (MRC1, red) and whole TAMs (F4/80, green) in 10- or 25-week-old TRAMP and TRAMP-Jα18$^{-/-}$ prostates. Nuclei were counterstained with DAPI (gray). The scale bars represent 50 μm; dashed yellow lines separate stromal and tumor areas.

(G) Quantification of TEMs per field. Dots indicate normalized MRC1 signal quantification in the imaged area. An average of 15 random non-overlapping fields per slide were analyzed in tissues from >3 independent mice per strain/age.

(H) Longitudinal quantification of data reported in (G).

Data in (A), (B), and (C) refer to one of two independent experiments performed with n = 3 and n = 4 mice per strain, giving comparable results. Graphs in (B), (E), (G), and (H) show mean ± SEM; statistical analysis by Student's two-tailed t test is shown.

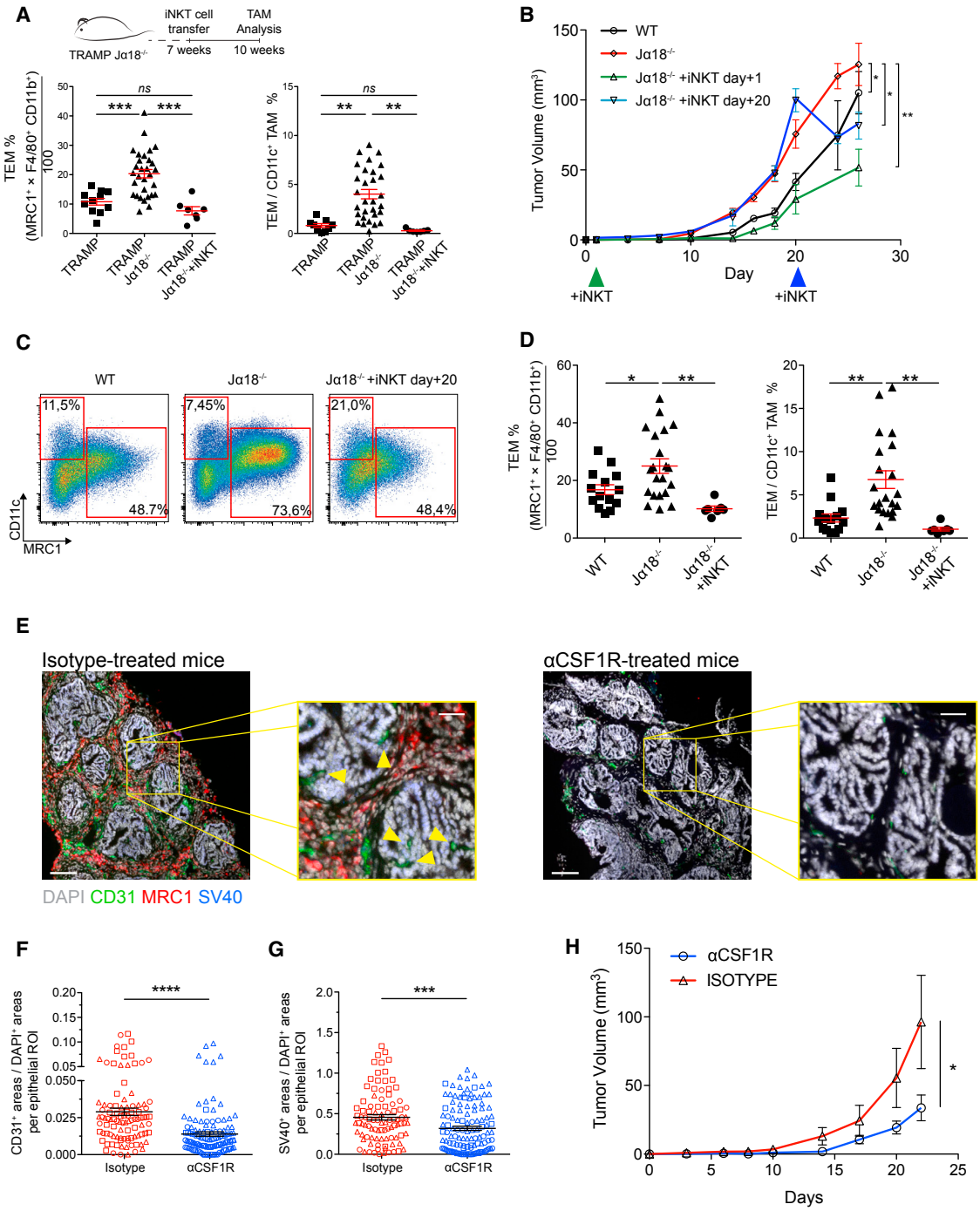

Figure 3. Transfer of iNKT Cells into Tumor-Bearing Animals Differentially Modulates TAM Populations and Delays Prostate Cancer Progression

(A) TEM frequency and TEM/CD11c$^+$ TAM ratio upon adoptive iNKT cell transfer. The experimental strategy is shown. Dots represent independent animals.

(B) Adoptive iNKT cell transfer in TRAMP-C1 tumor-bearing mice. Shown are the tumor growth curves in C57BL/6 mice (n = 9), Jα18$^{-/-}$ mice (n = 8), and Jα18$^{-/-}$ mice after adoptive iNKT cell transfer on day +1 (n = 5) or day +20 (n = 5).

(C) Representative flow cytometry plots of TEMs and CD11c$^+$ TAMs identified in TRAMP-C1 tumors single-cell suspensions explanted from indicated mice.

(D) Frequency of TEMs and TEM/CD11c$^+$ TAM ratio in TRAMP-C1 tumors grown in indicated mice. Dots represent independent animals.

(E) Immunostaining of prostate sections from TRAMP-Jα18$^{-/-}$ mice treated for 2 weeks with rat IgG2a control (n = 3) or anti-CSF1R mAb (n = 3) and stained for endothelium (CD31, green), TEMs (MRC1, red), and tumor cells (SV40, blue). Nuclei were counterstained with DAPI (gray). Arrowheads indicate tumor vascularization. The scale bars represent 100 μm (main images) or 50μm (boxed areas).

(legend continued on next page)

tumor angiogenesis, respectively (Crowe et al., 2002; Hayakawa et al., 2002). Finally, TAM killing by FasL-Fas engagement is the main cytolytic mechanism exerted by iNKT cells (Wingender et al., 2010).

MRC1$^+$ TEMs and CD11c$^+$ TAMs freshly isolated from TRAMP PCa expressed CD1d and CD40 to comparable levels, whereas Fas expression was slightly higher on TEMs than CD11c$^+$ TAMs (Figure S6). We also verified the expression of CD40L and FasL on iNKT cell subsets. iNKT1, 2, and 17 cells expressed CD40L to similar level, whereas FasL was mainly expressed on iNKT1 cells (Figures 5A and 5B).

To assess the contribution of CD1d recognition, hepatic iNKT cells sorted from C57BL6 mice were transferred into 7-week-old TRAMP-CD1d$^{-/-}$ recipients, and their prostates were collected 3 weeks later to analyze the frequency of TEMs and CD11c$^+$ TAMs. In the absence of CD1d recognition, adoptively transferred iNKT were unable to modulate TEM frequency and the TEM/CD11c$^+$ TAM ratio, which remained as high as in untreated TRAMP-CD1d$^{-/-}$ prostates (Figure 5C). In these experiments, CD1d was absent from all tissues. To determine whether iNKT cell activation and TAM modulation required CD1d expression on either tumor-infiltrating immune cells or cancer cells, we injected TRAMP-C1 cancer cells (Figure 5D), which naturally express CD1d as the primary TRAMP PCa cells (Nowak et al., 2010), into CD1d$^{-/-}$ or Jα18$^{-/-}$ animals. Although both CD1d$^{-/-}$ and Jα18$^{-/-}$ mice lack iNKT cells, Jα18$^{-/-}$ mice contain CD1d-positive tumor-infiltrating cells. After 24 hr, the mice received iNKT cells. Consistent with results shown in Figure 3B above, TRAMP-C1 tumors grew faster in either iNKT cell-deficient host than in WT animals (Figure 5E). However, the transferred iNKT cells could control tumor progression only in Jα18$^{-/-}$, but not in CD1d$^{-/-}$, mice (Figure 5E). Furthermore, iNKT cell transfer into tumor-bearing CD1d$^{-/-}$ mice failed to reduce TEM frequency and the TEM/CD11c$^+$ TAM ratio, unlike in Jα18$^{-/-}$ mice (Figure 5F), suggesting that CD1d expression on tumor-infiltrating cells is necessary to unleash iNKT cell modulation of TAMs.

To investigate the putative roles of CD40, IFNγ, and Fas in the iNKT-TAM communication, iNKT cells were sorted from CD40L$^{-/-}$, IFN$\gamma^{-/-}$, or FasL$^{-/-}$ mice and transferred into 7-week-old TRAMP-Jα18$^{-/-}$ mice. Transfer of CD40L$^{-/-}$ iNKT cells failed to reduce TEM frequency and the TEM/CD11c$^+$ ratio in the prostate of TRAMP-Jα18$^{-/-}$ mice (Figure 5G), pointing to a requisite role for the CD40L-CD40 axis in the modulation of TAMs by iNKT cells. Transfer of IFNγ-deficient iNKT cells instead decreased both parameters, albeit to a lower extent than WT iNKT cells (Figure 5G), suggesting that IFNγ produced by iNKT cells was only partly involved in modulating PCa-associated macrophages. Finally, FasL-deficient iNKT cells failed to modulate TAMs (Figure 5G), suggesting that FasL-Fas engagement was also critically required for the modulation of TAMs by iNKT cells.

Altogether, these results revealed that the differential modulation of TEMs and CD11c$^+$TAMs by iNKT cells critically depended on non-redundant mechanisms entailing CD1d recognition and CD40 and Fas engagement. Somewhat surprisingly, production of IFNγ by iNKT cells was not critical for modulating TAMs.

iNKT Cells Sustain M1 and Kill M2 Macrophages *In Vitro* through Cooperative CD1d, CD40, and Fas Engagement

MRC1$^+$ TEMs and CD11c$^+$ TAMs display gene expression signatures and phenotypic and functional characteristics partly reminiscent of bone marrow (BM)-derived macrophages polarized toward M1-like (M IFNγ) and M2-like (M IL-4) activation, respectively (Pucci et al., 2009). We therefore assessed the effects of coculturing BM-derived M1, M2, and unstimulated (M0) macrophages with iNKT cells expanded *in vitro* from the spleen of WT or FasL$^{-/-}$ mice. The 3 macrophage populations expressed CD1d, CD40, and Fas to similar levels (Figure 6A). Splenic iNKT cells could be activated *in vitro* to release cytokines in a CD1d-dependent manner by M1 and M2 macrophages loaded with αGalCer (Figure 6B). Upon coculture, however, iNKT cells protected M1 macrophages from death, whereas they selectively killed M2 macrophages in a CD1d-dependent manner (Figures 6C and 6D). iNKT cell protection of M1 cells critically depended on the expression of CD40 by macrophages, as CD40$^{-/-}$ M1 cells were killed by iNKT cells in the same setting (Figure 6E). By contrast, CD40 did not play an obvious role in M2 macrophages, as CD40$^{-/-}$ and WT M2 macrophages were both killed by iNKT cells upon CD1d recognition (Figures 6D and 6E). The selective killing of M2 macrophages by iNKT cells was instead dependent on FasL-Fas engagement, because FasL$^{-/-}$ iNKT cells failed to kill M2 macrophages (Figure 6F). Importantly, iNKT cells were also able to differentiate unstimulated M0 cells into M1 macrophages upon coculture *in vitro*. This property required CD1d cognate recognition, but not CD40 engagement (Figure 6G). Hence, iNKT cells differentially promoted survival and killing of M1-like and M2-like macrophages, respectively, via CD1d-cognate activation and the cooperative action between CD40L/CD40 and FasL/Fas molecules.

Reduced iNKT Cells and Increased TEM and Angiogenic Signatures Are Hallmarks of Aggressive Human PCa

We finally validated the clinical relevance of the iNKT/TAM cross-talk in human PCa. To this aim, we first compiled a gene signature specific for mouse TEMs using genes highly expressed in these cells (Pucci et al., 2009) and also present in our microarray data (67 out of 77 genes; Figure S7A). We then compared the gene signature in tumor-infiltrating CD45$^+$ cells of either TRAMP or TRAMP-Jα18$^{-/-}$. The analysis showed significant enrichment

(F and G) Signal quantification for (F) CD31$^+$ tumor vascular and (G) SV40$^+$ tumor cell areas. Dots indicate signal quantification in a single epithelial area. A minimum of 15 random non-overlapping fields was analyzed per mouse. Different symbols indicate independent animals.
(H) TRAMP-C1 tumor growth in WT animals that received anti-CSF1R (n = 6) or isotype control (n = 6) mAbs for three weeks.
(A) and (D) show cumulative results from all performed experiments. (B) shows the results from one representative experiment of three performed with reproducible results. Data in (A), (B), (D) and (F)–(H) are depicted as mean ± SEM. Statistical analysis by one-way ANOVA with Tukey post-test (A, B, and D) and Student's two-tailed t test (F, G, and H) is shown. For tumor growth (B and H), statistical analysis was performed on $\log_{10}$ of area under curve (AUC). See also Figure S2.

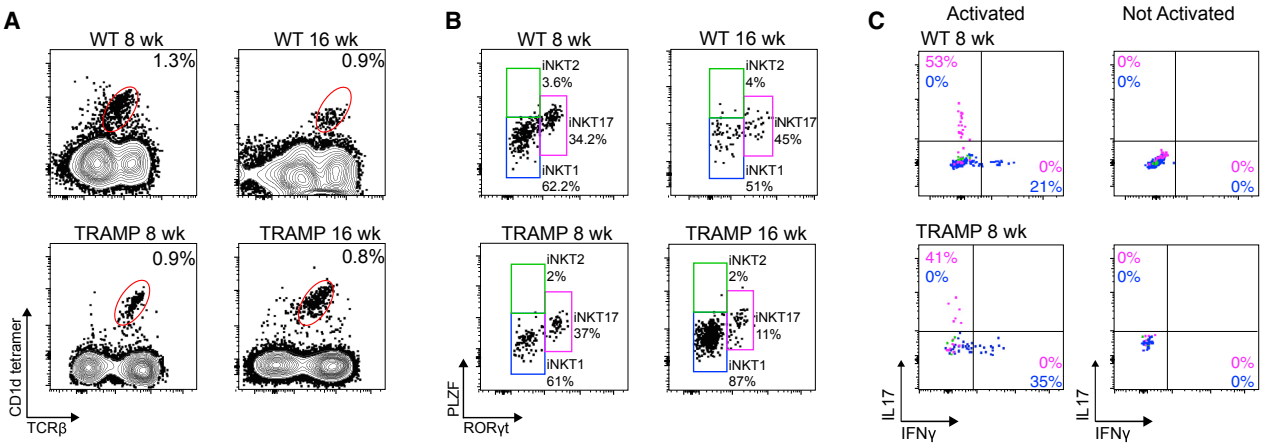

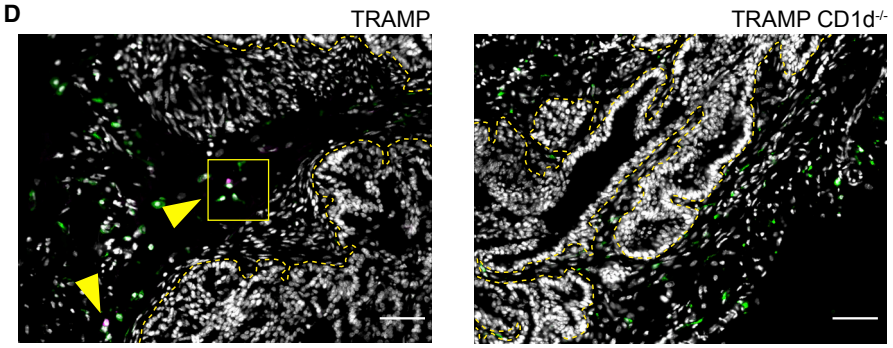

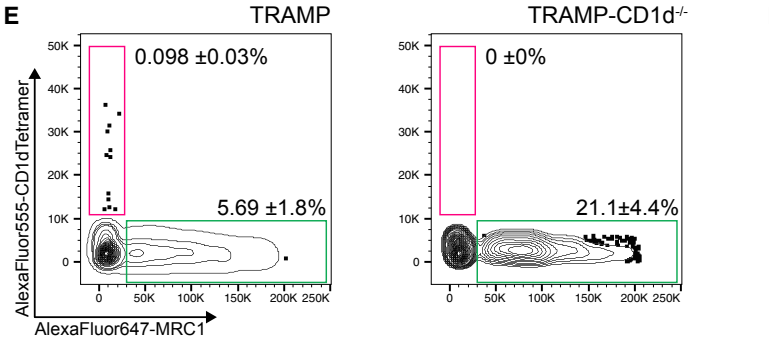

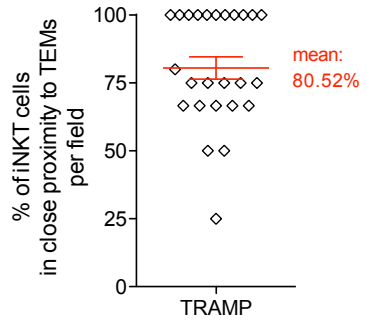

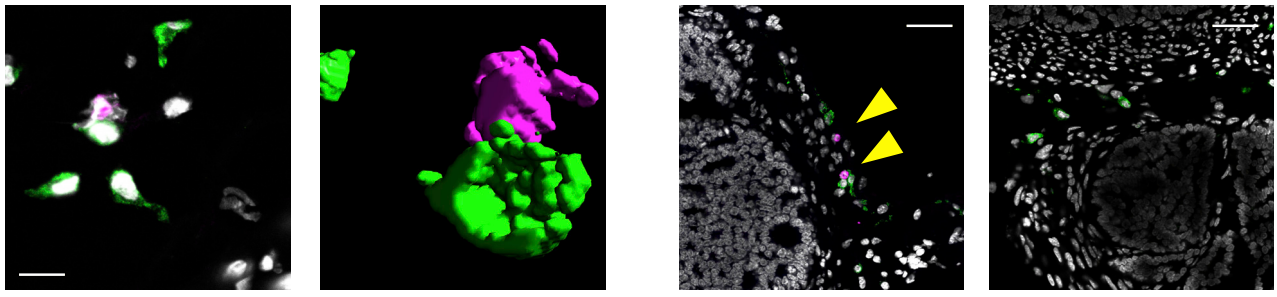

(legend on next page)

of the TEM gene signature in progressing tumors of iNKT cell-deficient TRAMP mice (Figure 7A), consistent with histology and flow cytometry, thus confirming the validity of the signature. We then ascertained the clinical relevance of these data in human PCa by investigating the distribution of the TEM signature in 191 primary PCa samples, whose gene expression and clinical data are available in the Genomic Data Commons (GDC) (Abeshouse et al., 2015). Patients were stratified according to low or high disease aggressiveness based on reviewed Gleason score, and remarkably, the expression of the TEM signature was significantly enriched in patients with higher tumor aggressiveness (Figures 7B and 7C). This was confirmed by immunostaining of human PCa with antibodies against the M2-associated markers CD163 (Figures 7D and 7E) and MRC1 (Figures 7F and 7G). Samples from patients with high Gleason score ($\geq$8) had a significant accumulation of M2-like TAMs compared to patients with lower aggressiveness (Figures 7E and 7G). We also detected significantly more iTCR^{+}CD3^{+} iNKT cells in the prostate of less aggressive low-Gleason-score patients compared to more aggressive high-Gleason-score specimens (Figures 7H and 7I), consistent with data obtained in the TRAMP model. CD3^{+} T cells were distributed similarly in low- and high-Gleason-score tumors (Figure 7J). Furthermore, the *hallmark angiogenesis* gene set was significantly enriched in human PCa samples with higher Gleason score compared to less aggressive tumors (Figures S7B and S7C), in agreement with data obtained in the TRAMP model. Together, these results support the notion that an inverse correlation exists between iNKT cell infiltration, the abundance of M2-like TAMs, and angiogenic blood vessels in human PCa.

DISCUSSION

This study underscores dichotomous CD40/Fas-dependent interactions between iNKT cells and TAMs, which control PCa progression in mouse tumor models. Both *in vivo* and *in vitro* experiments highlighted the critical involvement of non-redundant, cooperative engagement of CD1d, CD40, and Fas by iNKT cells to modulate the composition of PCa-associated macrophages. TEMs and CD11c^{+} TAMs expressed comparable levels of CD1d, CD40, and Fas and thus were equally susceptible to iNKT cell modulation via these molecules. The requirement for CD1d expression on TAMs implies the recognition of self-lipid antigens by iNKT cells, which may be induced in either TAM population upon stress-related environmental cues (Kain et al., 2014) or, alternatively, be synthetized in cancer cells and subsequently taken up by TAMs for cross-presentation to iNKT cells, as described in a human neuroblastoma model (Song et al., 2009). Our demonstration that CD40 engagement by iNKT cells protects M1, but not M2, macrophages from Fas-dependent killing strongly hints at a differential intersection of the two signaling pathways in the two macrophage subsets. We speculate that specific anti-apoptotic molecules recruited/induced in a CD40-dependent manner, such as cFLIP, could intervene in preventing Fas-driven apoptosis in M1, but not M2, macrophages. In addition, previous studies also found the CD40L/CD40 axis to be necessary for iNKT cell-dependent differentiation of immature myeloid precursors into stimulatory DCs (De Santo et al., 2008; Kitamura et al., 1999). We extend this notion by showing that CD40 engagement by iNKT cells is not required for the differentiation of unstimulated M0 macrophages into M1 cells, suggesting distinct CD40-dependent effects in macrophage and immature myeloid precursors, possibly depending on specific additional accessory signals. The production of IFNγ by iNKT cells was not critical for their antitumoral functions in the TRAMP model. This was surprising, given the prominent role of IFNγ in M1 macrophage induction (Murray et al., 2014). However, iNKT cells may indirectly stimulate IFNγ production by macrophages, DCs, CD8 T cells, and NK cells in the TME (Kitamura et al., 1999).

Our data lend strong support to the emerging concept that the interaction between iNKT cells and macrophages in tissues may represent a key function of these cells (Lynch et al., 2012, 2015; Smith et al., 2016). iNKT cell subsets with opposite effector functions localize in different organs, at least in mice, and can either promote inflammatory and tissue-disruptive M1-like macrophages (e.g., in cancer) or anti-inflammatory and tissue-remodeling M2-like macrophages (e.g., in the adipose tissue and large arteries; Lynch et al., 2012, 2015; Smith et al., 2016). This may have a critical impact on tissue pathophysiology, as functional defects acquired by iNKT cells in disease states may ultimately subvert macrophage activation contributing to tumor

Figure 4. iNKT Cells Localize at the Tumor Site

(A) Flow cytometry analysis of iNKT cells from the prostate of C57BL/6 (WT) and TRAMP mice at indicated ages. Data are obtained from pools of 5 prostates per mouse strain/age. One of two comparable experiments with the same n of mice is shown.

(B) Subset analysis of prostate-infiltrating iNKT cells shown in (A).

(C) Intracellular IL-17 and IFNγ production in iNKT cell subsets following *ex vivo* activation. The frequencies of cytokine-producing cells refer to iNKT1 (blue) or iNKT17 (magenta) gating.

(D) Representative immunostaining of prostate sections from indicated mice stained for iNKT cells (CD1d-tetramer, magenta) and TEMs (MRC1, green). Nuclei were counterstained with DAPI (gray). Arrowheads show iNKT cells in the stroma surrounding the tumor. Dashed yellow line separates stromal and epithelial areas. No CD1d-tetramer signal was detected in control TRAMP-CD1d$^{-/-}$ prostates. Tissues from 3 independent mice/strain were analyzed. The scale bars represent 50 μm.

(E) Representative histo-cytometry quantification of stained iNKT cells and TEM in the prostates of TRAMP and TRAMP-CD1d$^{-/-}$ mice. Graphs are obtained by concatenating data from 10 random non-overlapping fields per analyzed mouse. Fields from 3 independent mice per strain were quantified. Percentages indicate mean $\pm$ SD.

(F) Frequency (mean $\pm$ SEM) of iNKT cells detected adjacent to MRC1^{+} TEM by microscopy analysis of 3 independent mice.

(G) Confocal z stack plane of the boxed area in (D) shows direct contact between iNKT cells and MRC1^{+} macrophages. The scale bar represents 10 μm.

(H) 3D reconstruction of TEM-iNKT cell contact shown in (D) by z stack rendering.

(I) Confocal imaging of transferred iNKT cells (magenta) within the prostate of a 12-week-old TRAMP-Jα18$^{-/-}$ recipient. No CD1d-tetramer staining was detected in non-transferred age-matched TRAMP-Jα18$^{-/-}$ prostates. Tissues from 3 independent mice per treatment were analyzed.

See also Figures S3–S5.

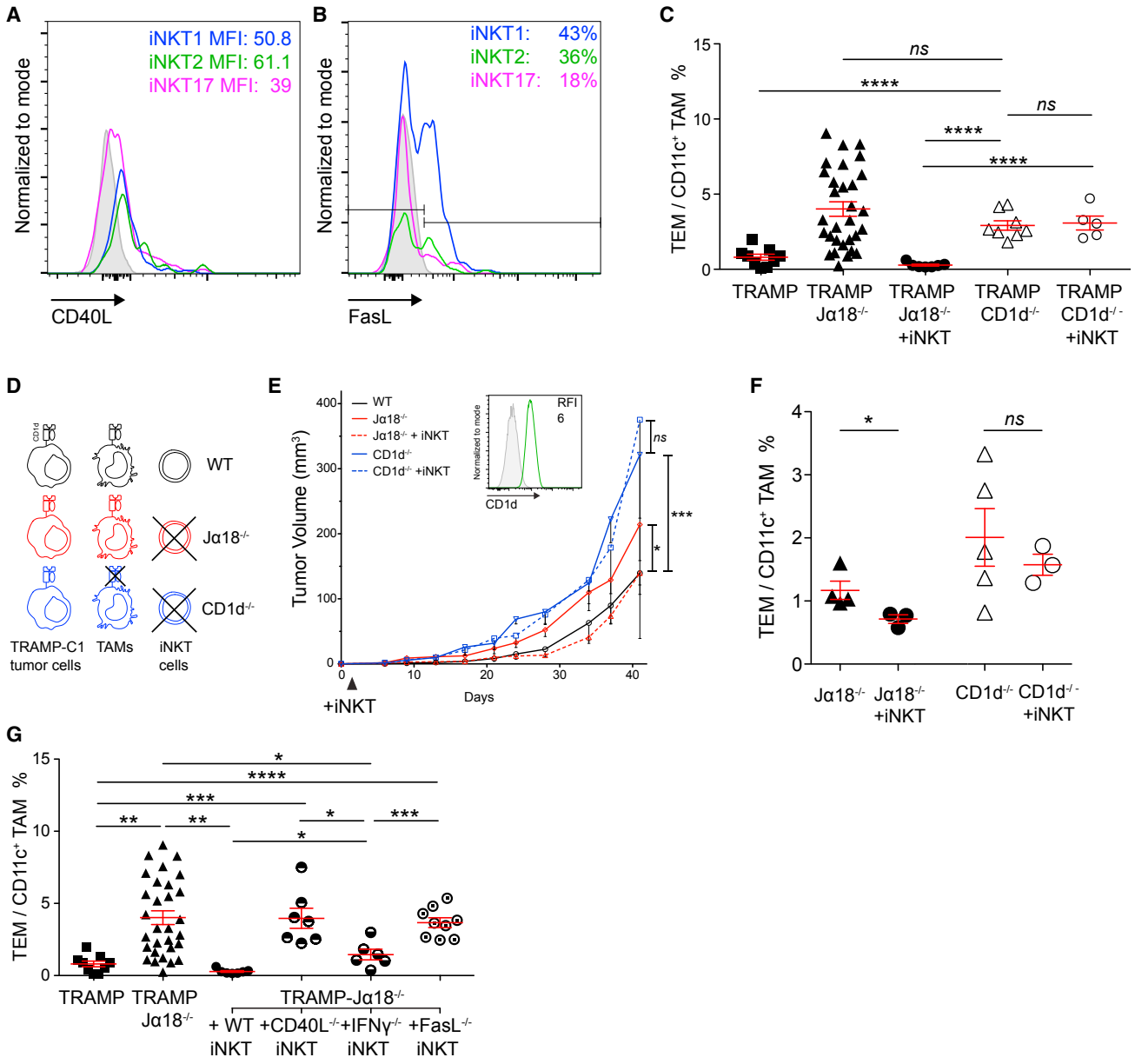

Figure 5. iNKT Cell Modulation of TAMs *In Vivo* Depends on CD1d Recognition and CD40L-CD40 and FasL-Fas Engagement

(A and B) Flow cytometry expression of (A) CD40L and (B) FasL on iNKT1/2/17 cell subsets gated as shown in Figures 4A and 4B. Grey histograms represent FMO controls.

(C) TEM/CD11c$^+$ TAM ratio determined in the indicated mice.

(D) Experimental scheme for tumor growth experiment reported in (E).

(E) Growth curves of subcutaneous (s.c.) TRAMP-C1 tumors in indicated mice, with (dotted line) or without (solid line) adoptive iNKT cell transfer at day +1. Depicted is one of three comparable experiments, performed with n = 10 mice per group. Inset shows CD1d expression on TRAMP-C1 cells (green) versus FMO (gray).

(F) TEM/CD11c$^+$ TAM ratio determined within s.c. TRAMP-C1 tumors dissected at day +40 from indicated mice.

(G) TEM/CD11c$^+$ TAM ratio in TRAMP, TRAMP-Jα18$^{-/-}$ and TRAMP-Jα18$^{-/-}$ prostates upon adoptive transfer of WT, CD40L$^{-/-}$, IFN$\gamma^{-/-}$ or FasL$^{-/-}$ iNKT cells.

(A), (B), (E), and (F) show results from one representative experiment of three performed with reproducible results. (C) and (G) show cumulative results from all performed experiments. Data in (C), and (E)–(G) are mean ± SEM. Dots represent independent animals. Statistical analysis by one-way ANOVA with Tukey post-test (C, E, and G) and Student's two-tailed t test (F). For (E), statistical analysis was performed on $\log_{10}$ of AUC. See also Figure S6.

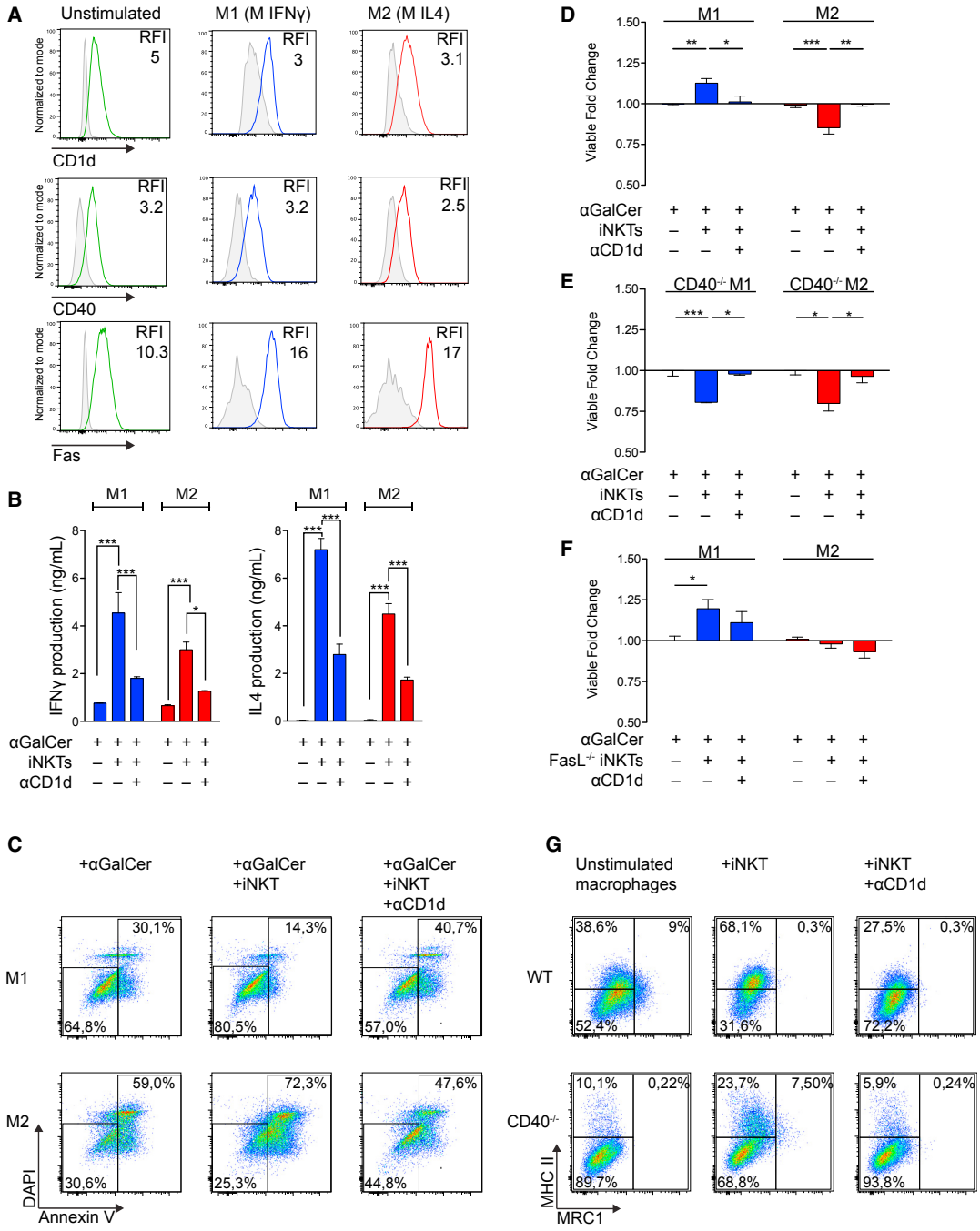

Figure 6. iNKT Cells Selectively Sustain M1 Macrophages via CD40 Engagement and Kill M2 Macrophages through Fas Ligation *In Vitro*

(A) Flow cytometry expression of CD1d, CD40, and Fas on indicated BM-derived macrophage populations. Grey histograms indicate FMO controls

(B) ELISA for IFNγ and IL-4 production in cocultures of αGalCer-loaded M1 or M2 cells with iNKT cells ± blocking CD1d mAb. The graphs show the mean of 3 independent experiments combined.

(C) Flow cytometry analysis of macrophage viability after 24 hr coculture with iNKT cells. Shown are representative plots from one of three independent experiments, each with up to four technical replicates per condition, which gave comparable results.

(D–F) Viability index of (D) WT M1 and M2 macrophages after 24 hr coculture with WT iNKT cells, (E) CD40$^{-/-}$ M1 and M2 macrophages after 24 hr coculture with WT iNKT cells, and (F) WT M1 and M2 BMDM after 24 hr coculture with FasL$^{-/-}$ iNKT cells. Graphs in (D)–(F) show combined data from three independent experiments, which gave comparable results.

(G) Representative flow cytometry plots of WT and CD40$^{-/-}$ unstimulated macrophages cultured alone or with iNKT cells ± blocking CD1d Ab. Data from one of two independent experiments are shown.

Data in (B), (D), (E), and (F) are shown as mean ± SEM. Statistical analysis by one-way ANOVA with Tukey post-test is shown.

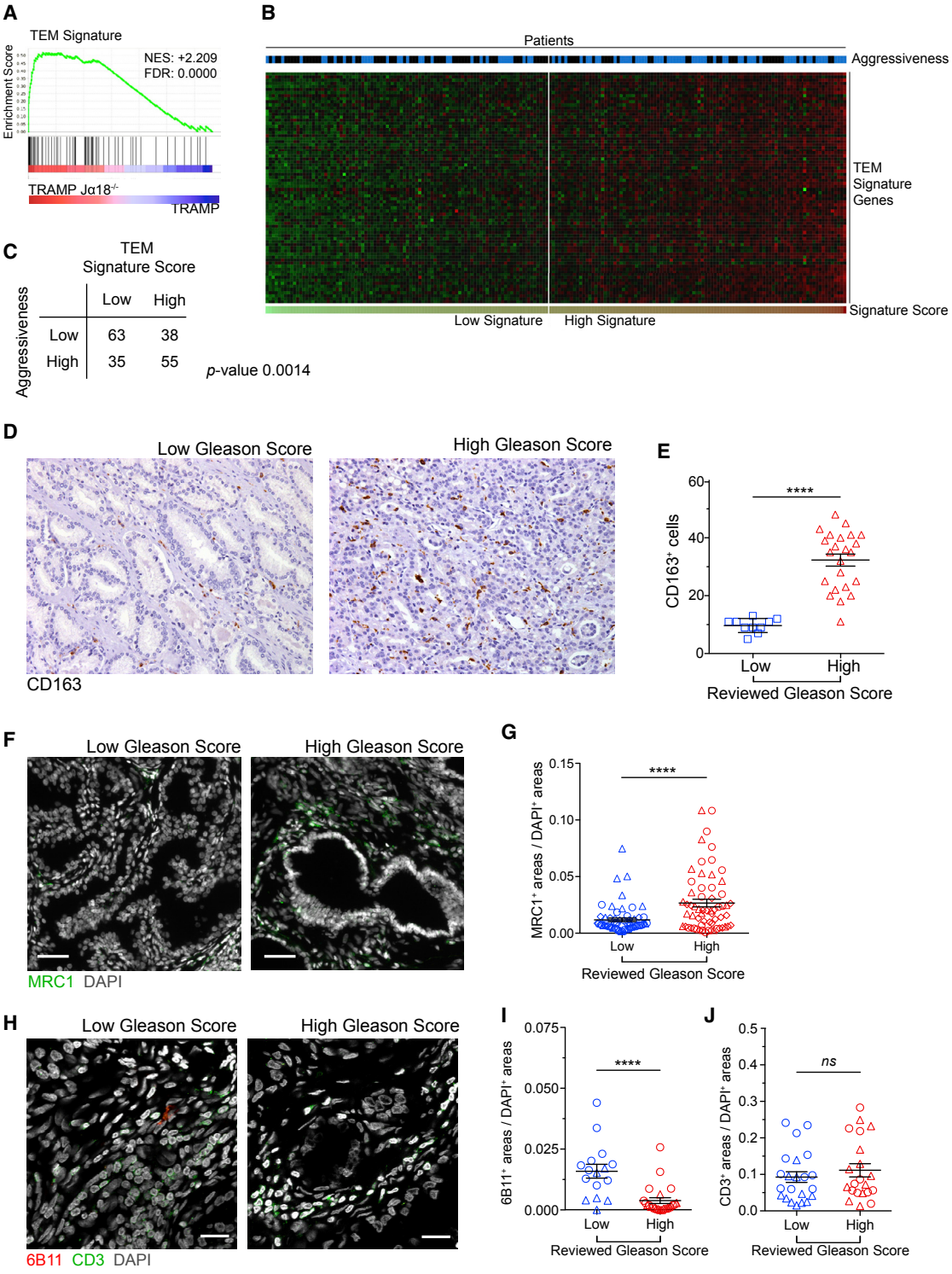

Figure 7. TEMs Expand in Patients with Aggressive PCa and Inversely Correlate with iNKT Cell Infiltration

(A) Enrichment plot of mouse TEM signature generated from published dataset (Pucci et al., 2009).

(B) Heatmap ordered from lower (left) to higher (right) TEM signature score (bar below) of human PCa samples from published dataset (Abeshouse et al., 2015). The vertical white line separates low from high TEM signature samples. For each patient, blue or black bars above the heatmap show high or low aggressiveness according to the reviewed Gleason score, respectively.

(C) Fisher's exact test between aggressiveness and TEM signature of human PCa.

(legend continued on next page)

progression or metabolic dysfunctions and atherosclerosis (Lynch et al., 2012, 2015; Smith et al., 2016). In this regard, we found that both TRAMP and healthy prostates contained a prevalent endogenous iNKT1 effector cell population, which was present in the prostate at steady state and displayed the type 1 effector functions required for tumor control. However, in selected organs where anti-inflammatory iNKT2 effector subsets predominate, such as the gut or lung, iNKT cells may well exhibit tumor-supporting functions, as recently suggested in a model of intestinal adenoma (Wang et al., 2018).

The expression of the human TEM signature, as well as of the pro-angiogenic gene set, significantly correlated with aggressiveness of human PCa, underscoring the preclinical relevance of results obtained in the mouse models and suggesting the involvement of pro-angiogenic TEMs in human disease progression. Accordingly, more aggressive human PCa contained increased M2-like ($CD163^+MRC1^+$) macrophages, accompanied by reduced iNKT cell infiltration. We were indeed able to detect iNKT cells infiltrating the human PCa stroma, although the presence and anatomical distribution of iNKT cells in human cancers has proven technically difficult to document as yet. Our data are consistent with the reduced representation of iNKT cells reported in the peripheral blood of advanced hormone-resistant PCa patients (Tahir et al., 2001). Detection, tissue localization and correlation with disease progression of macrophages in human and mouse PCa are unclear (Lissbrant et al., 2000; McClinton et al., 1990; Nonomura et al., 2011; Rigamonti et al., 2011; Shimura et al., 2000). Our analysis of human PCa is consistent with published evidence suggesting enrichment of alternatively activated $CD163^+$ M2-like macrophages, which are phenotypically overlapping with TEMs (Pucci et al., 2009), in advanced disease with poor prognosis (Comito et al., 2014; Lundholm et al., 2015). In agreement with mouse results, these data strongly suggest that the impairment of iNKT cells in aggressive human PCa, possibly combined with their reported acquisition of functional defects (Tahir et al., 2001), may affect TAM balance and promote angiogenesis, ultimately contributing to tumor progression.

Our results extend previous findings showing killing of tumor-infiltrating monocytes by human iNKT cells transferred to immunodeficient mice (Song et al., 2009). We have also recently shown that iNKT cells control chronic lymphocytic leukemia via modulation of M2-like nurse-like cells (Gorini et al., 2017), suggesting that TAM regulation by iNKT cells may modulate the progression of distinct cancer types.

iNKT cells are currently being investigated in clinical trials in both solid and hematological cancers, with promising results (Exley et al., 2017; Taniguchi et al., 2015). Our findings support their use in adoptive cell therapy settings for the therapeutic reprogramming of the TME in PCa and possibly other cancer types. The functional defects acquired by iNKT cells in progressing tumors, including PCa (Tahir et al., 2001), can be reverted by TCR-dependent activation and cytokines (IL-2 or IL-12) *in vitro* or *in vivo* (Nowak et al., 2010), suggesting that similar approaches may be used for enhancing iNKT cell activity also in advanced patients.

EXPERIMENTAL PROCEDURES

Study Design

This study was designed to investigate the role of iNKT cells in the spontaneous immunosurveillance to prostate cancer. To this aim, we took advantage of a spontaneous prostate cancer mouse model (TRAMP) and of mice that specifically lack iNKT cells ($J\alpha18^{-/-}$). Having elucidated that iNKT cells modulate two populations of TAMs, we addressed the underlying mechanisms by using specific knockout mice ($CD40L^{-/-}$, $CD40^{-/-}$, $CD1d^{-/-}$, $IFN\gamma^{-/-}$, and $FasL^{-/-}$). All procedures involving animals were reviewed and approved by the Institutional Animal Care and Use Committee (IACUC) (nos. 509 and 678) at the San Raffaele Scientific Institute. To validate these findings in the clinical setting, we performed immunostaining for critical markers on human PCa samples. All human tumor samples were obtained following informed consent of the patients, and their use for this study was reviewed and approved by the ethical committee at San Raffaele Hospital (protocol PROS-MAC-01).

Details on all performed experiments are described in the Supplemental Experimental Procedures. Donors of iNKT cells, mice used for bone-marrow-derived macrophages differentiation and for TRAMP-C1 subcutaneous tumor growth experiments were of 8 or 9 weeks of age. Unless otherwise specified, characterization of myelo-macrophage infiltration has always been performed on mice of 10 weeks of age. Information about the sample size and statistical methods is present in figure legends. Data were typically collected through multiple independent experiments as described in figure legends. For TRAMP-C1 tumor growth analysis and adoptive iNKT cell transfers experiments, investigators were blinded when assessing results. In some cases, selected samples were excluded from specific analysis because of technical flaws during sample processing or data acquisition.

Statistics

Comparisons between groups were performed using the two-tailed Student's t test with 95% confidence interval or using the 1-way ANOVA with Tukey post-test. Comparisons of TRAMP-C1 growth were performed on the area under curve (see Supplemental Information). Kaplan-Meier survival curves were analyzed by log rank (Mantel-Cox) test adjusted for multiple comparisons. Statistical computations were performed using GraphPad Prism v5.0. Over-representation analysis for the angiogenesis gene signature and TEM gene signature in the Cancer Genome Atlas (TCGA) dataset was performed using

(D) Immunohistochemistry (IHC) staining for M2-like TAMs (CD163) on low- and high-Gleason-score human PCa sections. Nuclei are counterstained by hematoxylin. 400× magnification images are shown.
(E) $CD163^+$ cells on IHC slides were counted and plotted according to reviewed Gleason score. Each dot represents a single patient and accounts for the average number of $CD163^+$ cells in 4 random, non-overlapping fields.
(F) Immunofluorescence (IF) analysis for M2-like TAMs (MRC1, green) on low- and high-Gleason-score human PCa sections. Nuclei were counterstained with DAPI (gray). The scale bar represents 50 μm.
(G) Quantification of TEMs per field. Graph shows the area occupied by MRC1 signal, normalized on the area with DAPI signal in the imaged tissue area. Each dot represents normalized signal quantification in the imaged area. An average of 20 fields per patient (n = 3 low and n = 3 high Gleason score, respectively) were analyzed. Different symbols indicate different patients.
(H) Confocal staining for invariant iNKT cells (invariant Vα24-Jα18 iTCR 6B11 mAb, red) and total T cells (CD3, green) on low- and high-Gleason-score human PCa sections. Nuclei were counterstained with DAPI (gray). The scale bar represents 20 μm.
(I and J) Sections were also acquired under fluorescence microscope and quantified for 6B11 (I) and CD3 (J) signal. An average of 10 fields per patient (n = 2 low and 2 high Gleason score, respectively) were analyzed. Different symbols indicate different patients.
In (E), (G), (I), and (J) data are depicted as mean ± SEM; statistical analysis by Student's two-tailed t test. See also Figure S7.

the Fisher's exact test by the fisher.test function in R. Statistical significance is as follows: *p < 0.05; **p ≤ 0.01; ***p ≤ 0.001; and ****p ≤ 0.0001.

DATA AND SOFTWARE AVAILABILITY

The accession number for the mouse microarray data reported in this paper is GEO: GSE94359.

SUPPLEMENTAL INFORMATION

Supplemental Information includes Supplemental Experimental Procedures and seven figures and can be found with this article online at https://doi.org/10.1016/j.celrep.2018.02.058.

ACKNOWLEDGMENTS

Alembic facility (San Raffaele Scientific Institute) is acknowledged for the support on imaging experiments. We are grateful to NIH tetramer facility for providing the mouse CD1d tetramers. Study was funded by Italian Ministry of Health (RF-2009-1531842) to M.B. and P.D., by Italian Association for Cancer Research-AIRC (IG 2014-15466 and IG 2014-15517) to P.D. and G.C., by AIRC Special Program Molecular Clinical Oncology "5 per mille" and Epigenetics Flagship project CNR-MIUR grants to S.B., and by an AIRC-FIRC Fellowship to F.C. (2015-18316). F.C. performed experiments of the study as fulfillment of his PhD degree of the International PhD School of Molecular Medicine, Università Vita-Salute San Raffaele, Milan, Italy.

AUTHOR CONTRIBUTIONS

Conceptualization, F.C., G.D., M.B., G.C., and P.D.; Methodology, F.C., G.D., A.G., S.B., M.B., G.C., and P.D.; Investigation, F.C., G.D., A.G., A.C., F.G., F.P., M.D.P., R.L., and M.G.; Resources, A.R., F.B., A.B., A.S., and C.D.; Writing – Drafting and Editing, F.C., G.D., G.C., and P.D.; Writing – Review, F.P., M.D.P., S.B., M.B., G.C., and P.D.; Supervision and Funding Acquisition, M.B., G.C., and P.D.

DECLARATION OF INTERESTS

The authors declare no competing interests.

Received: October 4, 2017
Revised: January 10, 2018
Accepted: February 13, 2018
Published: March 13, 2018

REFERENCES

Abeshouse, A., Ahn, J., Akbani, R., Ally, A., Amin, S., Andry, C.D., Annala, M., Aprikian, A., Armenia, J., Arora, A., et al.; Cancer Genome Atlas Research Network (2015). The molecular taxonomy of primary prostate cancer. Cell *163*, 1011–1025.

Baer, C., Squadrito, M.L., Laoui, D., Thompson, D., Hansen, S.K., Kiialainen, A., Hoves, S., Ries, C.H., Ooi, C.H., and De Palma, M. (2016). Suppression of microRNA activity amplifies IFN-γ-induced macrophage activation and promotes anti-tumour immunity. Nat. Cell Biol. *18*, 790–802.

Bassiri, H., Das, R., Guan, P., Barrett, D.M., Brennan, P.J., Banerjee, P.P., Wiener, S.J., Orange, J.S., Brenner, M.B., Grupp, S.A., and Nichols, K.E. (2014). iNKT cell cytotoxic responses control T-lymphoma growth in vitro and in vivo. Cancer Immunol. Res. *2*, 59–69.

Bellone, M., Ceccon, M., Grioni, M., Jachetti, E., Calcinotto, A., Napolitano, A., Freschi, M., Casorati, G., and Dellabona, P. (2010). iNKT cells control mouse spontaneous carcinoma independently of tumor-specific cytotoxic T cells. PLoS ONE *5*, e8646.

Brennan, P.J., Brigl, M., and Brenner, M.B. (2013). Invariant natural killer T cells: an innate activation scheme linked to diverse effector functions. Nat. Rev. Immunol. *13*, 101–117.

Comito, G., Giannoni, E., Segura, C.P., Barcellos-de-Souza, P., Raspollini, M.R., Baroni, G., Lanciotti, M., Serni, S., and Chiarugi, P. (2014). Cancer-associated fibroblasts and M2-polarized macrophages synergize during prostate carcinoma progression. Oncogene *33*, 2423–2431.

Cortez-Retamozo, V., Etzrodt, M., Newton, A., Rauch, P.J., Chudnovskiy, A., Berger, C., Ryan, R.J.H., Iwamoto, Y., Marinelli, B., Gorbatov, R., et al. (2012). Origins of tumor-associated macrophages and neutrophils. Proc. Natl. Acad. Sci. USA *109*, 2491–2496.

Crowe, N.Y., Smyth, M.J., and Godfrey, D.I. (2002). A critical role for natural killer T cells in immunosurveillance of methylcholanthrene-induced sarcomas. J. Exp. Med. *196*, 119–127.

de Lalla, C., Rinaldi, A., Montagna, D., Azzimonti, L., Bernardo, M.E., Sangalli, L.M., Paganoni, A.M., Maccario, R., Di Cesare-Merlone, A., Zecca, M., et al. (2011). Invariant NKT cell reconstitution in pediatric leukemia patients given HLA-haploidentical stem cell transplantation defines distinct CD4+ and CD4- subset dynamics and correlates with remission state. J. Immunol. *186*, 4490–4499.

De Palma, M., Biziato, D., and Petrova, T.V. (2017). Microenvironmental regulation of tumour angiogenesis. Nat. Rev. Cancer *17*, 457–474.

De Santo, C., Salio, M., Masri, S.H., Lee, L.Y.-H., Dong, T., Speak, A.O., Porubsky, S., Booth, S., Veerapen, N., Besra, G.S., et al. (2008). Invariant NKT cells reduce the immunosuppressive activity of influenza A virus-induced myeloid-derived suppressor cells in mice and humans. J. Clin. Invest. *118*, 4036–4048.

De Santo, C., Arscott, R., Booth, S., Karydis, I., Jones, M., Asher, R., Salio, M., Middleton, M., and Cerundolo, V. (2010). Invariant NKT cells modulate the suppressive activity of IL-10-secreting neutrophils differentiated with serum amyloid A. Nat. Immunol. *11*, 1039–1046.

Dhodapkar, M.V., Geller, M.D., Chang, D.H., Shimizu, K., Fujii, S., Dhodapkar, K.M., and Krasovsky, J. (2003). A reversible defect in natural killer T cell function characterizes the progression of premalignant to malignant multiple myeloma. J. Exp. Med. *197*, 1667–1676.

Exley, M.A., Friedlander, P., Alatrakchi, N., Vriend, L., Yue, S., Sasada, T., Zeng, W., Mizukami, Y., Clark, J., Nemer, D., et al. (2017). Adoptive transfer of invariant NKT cells as immunotherapy for advanced melanoma: a phase I clinical trial. Clin. Cancer Res. *23*, 3510–3519.

Franklin, R.A., Liao, W., Sarkar, A., Kim, M.V., Bivona, M.R., Liu, K., Pamer, E.G., and Li, M.O. (2014). The cellular and molecular origin of tumor-associated macrophages. Science *344*, 921–925.

Gabrilovich, D.I., Ostrand-Rosenberg, S., and Bronte, V. (2012). Coordinated regulation of myeloid cells by tumours. Nat. Rev. Immunol. *12*, 253–268.

Godfrey, D.I., Pellicci, D.G., Patel, O., Kjer-Nielsen, L., McCluskey, J., and Rossjohn, J. (2010). Antigen recognition by CD1d-restricted NKT T cell receptors. Semin. Immunol. *22*, 61–67.

Gorini, F., Azzimonti, L., Delfanti, G., Scarfò, L., Scielzo, C., Bertilaccio, M.T., Ranghetti, P., Gulino, A., Doglioni, C., Di Napoli, A., et al. (2017). Invariant NKT cells contribute to chronic lymphocytic leukemia surveillance and prognosis. Blood *129*, 3440–3451.

Greenberg, N.M., DeMayo, F., Finegold, M.J., Medina, D., Tilley, W.D., Aspinall, J.O., Cunha, G.R., Donjacour, A.A., Matusik, R.J., and Rosen, J.M. (1995). Prostate cancer in a transgenic mouse. Proc. Natl. Acad. Sci. USA *92*, 3439–3443.

Hanahan, D., and Coussens, L.M. (2012). Accessories to the crime: functions of cells recruited to the tumor microenvironment. Cancer Cell *21*, 309–322.

Hanahan, D., and Weinberg, R.A. (2011). Hallmarks of cancer: the next generation. Cell *144*, 646–674.

Hayakawa, Y., Takeda, K., Yagita, H., Kakuta, S., Iwakura, Y., Van Kaer, L., Saiki, I., and Okumura, K. (2001). Critical contribution of IFN-gamma and NK cells, but not perforin-mediated cytotoxicity, to anti-metastatic effect of alpha-galactosylceramide. Eur. J. Immunol. *31*, 1720–1727.

Hayakawa, Y., Takeda, K., Yagita, H., Smyth, M.J., Van Kaer, L., Okumura, K., and Saiki, I. (2002). IFN-gamma-mediated inhibition of tumor angiogenesis by natural killer T-cell ligand, alpha-galactosylceramide. Blood *100*, 1728–1733.

Hermans, I.F., Silk, J.D., Gileadi, U., Salio, M., Mathew, B., Ritter, G., Schmidt, R., Harris, A.L., Old, L., and Cerundolo, V. (2003). NKT cells enhance CD4+ and CD8+ T cell responses to soluble antigen in vivo through direct interaction with dendritic cells. J. Immunol. *171*, 5140–5147.

Kain, L., Webb, B., Anderson, B.L., Deng, S., Holt, M., Costanzo, A., Zhao, M., Self, K., Teyton, A., Everett, C., et al. (2014). The identification of the endogenous ligands of natural killer T cells reveals the presence of mammalian α-linked glycosylceramides. Immunity *41*, 543–554.

Kitamura, H., Iwakabe, K., Yahata, T., Nishimura, S., Ohta, A., Ohmi, Y., Sato, M., Takeda, K., Okumura, K., Van Kaer, L., et al. (1999). The natural killer T (NKT) cell ligand alpha-galactosylceramide demonstrates its immunopotentiating effect by inducing interleukin (IL)-12 production by dendritic cells and IL-12 receptor expression on NKT cells. J. Exp. Med. *189*, 1121–1128.

Lewis, C.E., Harney, A.S., and Pollard, J.W. (2016). The multifaceted role of perivascular macrophages in tumors. Cancer Cell *30*, 18–25.

Lissbrant, I.F., Stattin, P., Wikstrom, P., Damber, J.E., Egevad, L., and Bergh, A. (2000). Tumor associated macrophages in human prostate cancer: relation to clinicopathological variables and survival. Int. J. Oncol. *17*, 445–451.

Lundholm, M., Hägglöf, C., Wikberg, M.L., Stattin, P., Egevad, L., Bergh, A., Wikström, P., Palmqvist, R., and Edin, S. (2015). Secreted factors from colorectal and prostate cancer cells skew the immune response in opposite directions. Sci. Rep. *5*, 15651.

Lynch, L., Nowak, M., Varghese, B., Clark, J., Hogan, A.E., Toxavidis, V., Balk, S.P., O'Shea, D., O'Farrelly, C., and Exley, M.A. (2012). Adipose tissue invariant NKT cells protect against diet-induced obesity and metabolic disorder through regulatory cytokine production. Immunity *37*, 574–587.

Lynch, L., Michelet, X., Zhang, S., Brennan, P.J., Moseman, A., Lester, C., Besra, G., Vomhof-Dekrey, E.E., Tighe, M., Koay, H.-F., et al. (2015). Regulatory iNKT cells lack expression of the transcription factor PLZF and control the homeostasis of T(reg) cells and macrophages in adipose tissue. Nat. Immunol. *16*, 85–95.

Mantovani, A., Sozzani, S., Locati, M., Allavena, P., and Sica, A. (2002). Macrophage polarization: tumor-associated macrophages as a paradigm for polarized M2 mononuclear phagocytes. Trends Immunol. *23*, 549–555.

McClinton, S., Miller, I.D., and Eremin, O. (1990). An immunohistochemical characterisation of the inflammatory cell infiltrate in benign and malignant prostatic disease. Br. J. Cancer *61*, 400–403.

Metelitsa, L.S., Wu, H.-W., Wang, H., Yang, Y., Warsi, Z., Asgharzadeh, S., Groshen, S., Wilson, S.B., and Seeger, R.C. (2004). Natural killer T cells infiltrate neuroblastomas expressing the chemokine CCL2. J. Exp. Med. *199*, 1213–1221.

Murray, P.J., Allen, J.E., Biswas, S.K., Fisher, E.A., Gilroy, D.W., Goerdt, S., Gordon, S., Hamilton, J.A., Ivashkiv, L.B., Lawrence, T., et al. (2014). Macrophage activation and polarization: nomenclature and experimental guidelines. Immunity *41*, 14–20.

Nakagawa, R., Nagafune, I., Tazunoki, Y., Ehara, H., Tomura, H., Iijima, R., Motoki, K., Kamishohara, M., and Seki, S. (2001). Mechanisms of the antimetastatic effect in the liver and of the hepatocyte injury induced by alpha-galactosylceramide in mice. J. Immunol. *166*, 6578–6584.

Nonomura, N., Takayama, H., Nakayama, M., Nakai, Y., Kawashima, A., Mukai, M., Nagahara, A., Aozasa, K., and Tsujimura, A. (2011). Infiltration of tumour-associated macrophages in prostate biopsy specimens is predictive of disease progression after hormonal therapy for prostate cancer. BJU Int. *107*, 1918–1922.

Nowak, M., Arredouani, M.S., Tun-Kyi, A., Schmidt-Wolf, I., Sanda, M.G., Balk, S.P., and Exley, M.A. (2010). Defective NKT cell activation by CD1d+ TRAMP prostate tumor cells is corrected by interleukin-12 with α-galactosylceramide. PLoS ONE *5*, e11311.

Noy, R., and Pollard, J.W. (2014). Tumor-associated macrophages: from mechanisms to therapy. Immunity *41*, 49–61.

Pucci, F., Venneri, M.A., Biziato, D., Nonis, A., Moi, D., Sica, A., Di Serio, C., Naldini, L., and De Palma, M. (2009). A distinguishing gene signature shared by tumor-infiltrating Tie2-expressing monocytes, blood "resident" monocytes, and embryonic macrophages suggests common functions and developmental relationships. Blood *114*, 901–914.

Renukaradhya, G.J., Khan, M.A., Vieira, M., Du, W., Gervay-Hague, J., and Brutkiewicz, R.R. (2008). Type I NKT cells protect (and type II NKT cells suppress) the host's innate antitumor immune response to a B-cell lymphoma. Blood *111*, 5637–5645.

Rigamonti, N., Capuano, G., Ricupito, A., Jachetti, E., Grioni, M., Generoso, L., Freschi, M., and Bellone, M. (2011). Modulators of arginine metabolism do not impact on peripheral T-cell tolerance and disease progression in a model of spontaneous prostate cancer. Clin. Cancer Res. *17*, 1012–1023.

Schneiders, F.L., de Bruin, R.C.G., van den Eertwegh, A.J.M., Scheper, R.J., Leemans, C.R., Brakenhoff, R.H., Langendijk, J.A., Verheul, H.M.W., de Gruijl, T.D., Molling, J.W., and van der Vliet, H.J. (2012). Circulating invariant natural killer T-cell numbers predict outcome in head and neck squamous cell carcinoma: updated analysis with 10-year follow-up. J. Clin. Oncol. *30*, 567–570.

Shimura, S., Yang, G., Ebara, S., Wheeler, T.M., Frolov, A., and Thompson, T.C. (2000). Reduced infiltration of tumor-associated macrophages in human prostate cancer: association with cancer progression. Cancer Res. *60*, 5857–5861.

Smith, E., Croca, S., Waddington, K.E., Sofat, R., Griffin, M., Nicolaides, A., Isenberg, D.A., Torra, I.P., Rahman, A., and Jury, E.C. (2016). Cross-talk between iNKT cells and monocytes triggers an atheroprotective immune response in SLE patients with asymptomatic plaque. Sci. Immunol. *1*, eaah4081.

Song, L., Asgharzadeh, S., Salo, J., Engell, K., Wu, H.-W., Sposto, R., Ara, T., Silverman, A.M., DeClerck, Y.A., Seeger, R.C., and Metelitsa, L.S. (2009). Valpha24-invariant NKT cells mediate antitumor activity via killing of tumor-associated macrophages. J. Clin. Invest. *119*, 1524–1536.

Squadrito, M.L., Pucci, F., Magri, L., Moi, D., Gilfillan, G.D., Ranghetti, A., Casazza, A., Mazzone, M., Lyle, R., Naldini, L., and De Palma, M. (2012). miR-511-3p modulates genetic programs of tumor-associated macrophages. Cell Rep. *1*, 141–154.

Swann, J.B., Uldrich, A.P., van Dommelen, S., Sharkey, J., Murray, W.K., Godfrey, D.I., and Smyth, M.J. (2009). Type I natural killer T cells suppress tumors caused by p53 loss in mice. Blood *113*, 6382–6385.

Tachibana, T., Onodera, H., Tsuruyama, T., Mori, A., Nagayama, S., Hiai, H., and Imamura, M. (2005). Increased intratumor Valpha24-positive natural killer T cells: a prognostic factor for primary colorectal carcinomas. Clin. Cancer Res. *11*, 7322–7327.

Tahir, S.M., Cheng, O., Shaulov, A., Koezuka, Y., Bubley, G.J., Wilson, S.B., Balk, S.P., and Exley, M.A. (2001). Loss of IFN-gamma production by invariant NK T cells in advanced cancer. J. Immunol. *167*, 4046–4050.

Taniguchi, M., Harada, M., Dashtsoodol, N., and Kojo, S. (2015). Discovery of NKT cells and development of NKT cell-targeted anti-tumor immunotherapy. Proc. Jpn. Acad., Ser. B, Phys. Biol. Sci. *91*, 292–304.

Wang, Y., Sedimbi, S., Löfbom, L., Singh, A.K., Porcelli, S.A., and Cardell, S.L. (2018). Unique invariant natural killer T cells promote intestinal polyps by suppressing TH1 immunity and promoting regulatory T cells. Mucosal Immunol. *11*, 131–143.

Wingender, G., Krebs, P., Beutler, B., and Kronenberg, M. (2010). Antigen-specific cytotoxicity by invariant NKT cells in vivo is CD95/CD178-dependent and is correlated with antigenic potency. J. Immunol. *185*, 2721–2729.